An innovative maximum power point tracking for photovoltaic systems operating under partially shaded conditions using Grey Wolf Optimization algorithm

Muhannad J. Alshareef

Published online: 08 Sep 2024.

Submit your article to this journal ⬏

Article views: 375

View related articles ⬏

View Crossmark data ⬏

Citing articles: 1 View citing articles ⬏

OPEN ACCESS

Check for updates

An innovative maximum power point tracking for photovoltaic systems operating under partially shaded conditions using Grey Wolf Optimization algorithm

Muhannad J. Alshareef

Department of Electrical Engineering, College of Engineering and Computing in Al-Qunfudhah, Umm Al-Qura University, Mecca, Saudi Arabia

ABSTRACT

Partial shading conditions (PSCs) may be unpredictable and difficult to forecast in large-scale solar photovoltaic (PV) systems. Potentially degrading the PV system's performance results from numerous peaks in the P–V curve caused by PSC. On the other hand, the PV system must be run at its maximum power point (GMPP) to maximize its efficiency. Swarm optimization strategies have been employed to detect the GMPP; however, these methods are associated with an unacceptable amount of time to reach convergence. In this research, an innovative grey wolf optimization, abbreviated as NGWO, is presented as a solution to overcome the shortcomings of the standard GWO method, which includes long conversion times, a rate of failure, and large oscillations in a steady-state condition. This paper seeks to address these issues and fill a gap in research by enhancing the GWO's performance in tracking GMPP. The original GWO is modified to incorporate the Cuckoo Search (CS) abandoned process to shorten the time it takes for effective adoption. Based on the simulation finding, the proposed IGWO method beats other algorithms in most circumstances, particularly regarding tracking time and efficiency, where the average tracking time is 0.19s, and the average efficiency is 99.86%.

1. Introduction

1.1. Motivation and incitement

Modern power grids increasingly view solar photovoltaic (PV) as their most promising energy source [1]. With global energy demand rising, skyrocketing fossil fuel costs and mounting environmental concerns, there has been a surge in interest in renewable energy sources. Recent years have seen significant increases in photovoltaic energy generation, leading to greater utilization of solar energy. PV systems offer the benefits of minimal maintenance costs, absence of operating or rotating parts, and pollution-free operation [1,2]. Many countries have rapidly expanded PV power generation systems through feed-in tariffs, subsidized programmes and more. However, PV power generating systems are often criticized for their poor energy conversion efficiency and high costs. Consequently, they are frequently optimized to harvest the maximum amount of power possible from the PV source. Maximum Power Point Tracking (MPPT) is a common method for optimizing the use of PV systems, involving a DC-DC converter or an inverter. MPPT aims to maximize the power extracted from PV systems under varying temperatures and irradiation levels. Given that both solar irradiation and temperature affect the PV curves, the MPPT process becomes more complex. Parallel and series connections of PV panels are often used to meet the power requirements of the load. When the weather changes, the location of the PV system's MPP shifts, and several MPPT algorithms have been proposed to detect it, as documented in references [3–9]. This list includes techniques like open-circuit voltage, Perturb and Observe (P&O), and Incremental Conductance (IC) methods. The study comprehensively reviews various strategies for detecting MPP in PV systems. Suppose the P–V curve has just one MPP during typical uniform irradiation conditions. The tracking methods described in these studies have been shown to be reliable and to provide a satisfactory rate of tracking.

The P–V curve of a PV system operating in PSCs has numerous peaks, and for optimal power extraction, the system must converge to its global maximum power point (GMPP). As a general rule, a low-cost digital controller is required to implement an MPPT algorithm that has simple computing steps, quicker convergence and a certain converge to GMPP.

CONTACT Muhannad J. Alshareef ✉ mjshareef@uqu.edu.sa ▣ Department of Electrical Engineering, College of Engineering and Computing in Al-Qunfudhah, Umm Al-Qura University, Mecca 24382, Saudi Arabia

1.2. Research gap

Several MPPT (Maximum Power Point Tracking) strategies have been developed to locate the global MPP under Partial Shading Conditions (PSCs) [10]. More complex approaches, such as fuzzy logic and Artificial Neural Networks (ANNs), require substantial data for control purposes. Examples of swarm intelligence algorithms used for GMPP tracking include Particle Swarm Optimization (PSO) [11–13], Artificial Bee Colony (ABC) algorithm [14], Firefly algorithm [15], Grey Wolf Optimization (GWO) [16] and the Bat algorithm [17]. PSO and its variants are particularly noted for their simplicity in design and implementation [11]. A multi-module PV system featuring numerous converters was designed using a PSO-based centralized MPPT controller. An MPPT strategy that relies on the PSO algorithm was implemented to control the duty cycle directly, minimizing the need for proportional–integral control loops in Pulse Width Modulation (PWM) signals [12]. Standard PSO for MPPT presents two main drawbacks due to significant divergence from high-velocity updated particles and extended convergence times with low-velocity particles. Study in [18] and [13] give suggestions for addressing these issues. Linearly increasing social parameter whereas, linearly lowering cognitive parameter and inertia weight was utilized to adjust the standard PSO in [18]. A reduction in the iterations needed to attain the GMPP was found to be the result of making some modifications but this increases the complexity of the algorithm.

In [19–21], two-stage algorithm integrates into the first stage swarm intelligence algorithm for capability to search globally, and P&O method is integrated into the second stage, which merges the local search ability, and uses MPPT control under PSCs. However, the P&O method can oscillate around the GMPP, which may result in degradation of PV efficiency.

In [22], the Artificial Bee Colony (ABC) algorithm was employed to determine the Global Maximum Power Point (GMPP) under Partial Shading (PS) conditions, showing superior convergence compared to the Particle Swarm Optimization (PSO) method. Nonetheless, the ABC algorithm tends to get stuck in a Local Maximum Power Point (LMPP) when operating with a limited number of bees. Another technique, the Ant Colony Optimization (ACO), as developed by [23], exhibits performance comparable to PSO under both uniform and varying shade conditions. Meanwhile, study in [24] introduced an enhanced differential evolution strategy to attain GMPP under PS, offering rapid convergence and straightforward deployment because of its minimal control parameters. However, this method lacks a mechanism to recall past particle movements and locations, making it prone to becoming trapped at local maxima.

Grey wolf optimization (GWO) was first utilized in a PV generation system as noted in [16,25], yet it encounters inherent challenges that can extend the search duration. In [26], GWO is merged with the perturb and observe (P&O) method to achieve quicker convergence. Nonetheless, the characteristics of P&O can lead to undesirable steady-state power oscillations. Study in [27] enhanced the performance of GWO by adjusting the balance between exploration and exploitation phases. However, introducing additional parameters can complicate the system further.

Slap swarm algorithm (SSA) and GWO are combined to create the MPPT controller [28]. The GWO method's leadership structure is included in the standard SSA algorithm to improve global search capabilities. The starting value of the crow search algorithm (CSA), according [29], should be set to the ideal duty ratio as found by GWO.

Additionally, a technique for determining the DC impedance of a PV string using GWO is presented to prevent extreme local problems [30]. The cuckoo search (CS) was first introduced in the year 2009 [31], which was influenced by the brooding habits of Cuckoos. The method proved to be more effective than PSO [21,32–34]. However, the convergence speed of CS is influenced by the Lévy flight, which can result in slower convergence.

The enhanced GWO method developed in [35] removes the (δ) and (ω) wolves from the standard GWO algorithm to simplify the computation process and is directly utilized for PV generating systems to monitor the GMPP. However, eliminating the δ and ω wolves, which contribute toward GMPP, may cause the algorithm to become trapped at local MPP under complex partial shading conditions. This method has better speed of tracking and good accuracy in comparison to the other methods. As a result, EGWO will be utilized to compare to the method proposed here.

1.3. Contribution

The primary aim of this research is to enhance the functionality of the conventional Grey Wolf Optimization (GWO) method by decreasing tracking time and improving efficiency. This is achieved by integrating the abandoning mechanism from Cuckoo Search (CS) into the GWO, resulting in the proposed Modified Novel Grey Wolf Optimization (NGWO). The simulation results show that this method significantly improves convergence time and accuracy. The structure of this paper is as follows: Section 2 provides an overview of photovoltaic (PV) modelling in partial shading conditions. Section 3 outlines the Conventional GWO. Section 4 details the proposed NGWO algorithm and its application in Maximum Power Point Tracking (MPPT) for PV systems. The results and discussion
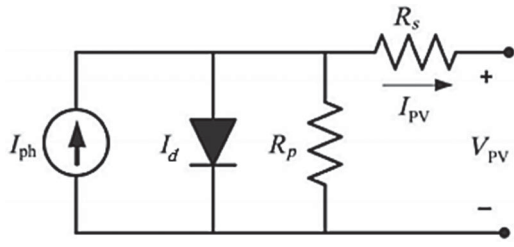
Figure 1. Model of a solar cell.

of the simulations are presented in Section 5. Finally, Section 6 summarizes the findings.

2. Characteristics of photovoltaic array

2.1. The photovoltaic cell model

Figure 1 depicts the PV cell's equivalent circuit. The incoming light (G) can produce current I_{PV}, I_d is the diode's forward bias current, and R_P and R_S denote the cell's inherent shunt and series resistance, correspondingly. It is possible to represent mathematically the relationship that exists between the current (I) and voltage (V) of the PV solar cell as follow:

$$I = I_{PV} - I_O \left\{ exp \left[\frac{q(V + IR_S)}{nKT} \right] - 1 \right\} - \frac{V + IR_S}{R_P} \tag{1}$$

Where PV current, leakage current, are denoted by I_{ph} and I_o, respectively. The reverse saturation current of a diode is depicted by the I_O, K is the constant of Boltzmann, the temperature is expressed in kelvins as T, q denotes the charge of an electron, the diode ideality constant is denoted by n, while the diode cross-voltage is denoted by the voltage $V + IR_s$.

Under three different scenarios (open circuit, short circuit and maximum power point), the information included in the datasheet may be used to derive the five parameters of the circuit model (I_{PV}, I_0, R_S and R_P), which are referred as collectively as [36]. As a consequence of this, the following are the finding obtained by substituting the parameters of the maximum power point ($V = V_{mpp}$, $I = I_{mpp}$), the open circuit ($V = V_{OC}$, $I = 0$), the short circuit ($V = 0$, I_{SC}), conditions into (1):

$$0 = I_{PV} - I_O \left[exp \left(\frac{qV_{OC}}{nKT} \right) - 1 \right] - \frac{V_{OC}}{R_P} \tag{2}$$

$$I_{SC} = I_{PV} - I_O \left[exp \left(\frac{qI_{SC}R_S}{nKT} \right) - 1 \right] - \frac{I_{SC}R_S}{R_P} \tag{3}$$

$$I_{sc} = I_{PV} - I_O \left\{ exp \left[\frac{q(V_{MPP} + I_{MPP}R_S)}{nKT} \right] - 1 \right\}$$
$$- \frac{V_{MPP} + I_{MPP}R_S}{R_P} \tag{4}$$

I_{SC} indicates short-circuit current, V_{OC} stands for open circuit voltage, I_{MPP} refers to current at maximum

power point and V_{MPP} stands for maximum power point voltage. When building practical devices, the shunt resistance R_P is usually large enough to ignore. R_S's value may also be found in the datasheet, as well. It is also possible to extract additional circuit model unknown parameters using (2)–(4).

2.2. Irradiance and temperature effects

A standard test condition (STC) is defined as an irradiation of 1000 W/m^2, a cell temperature of 25°C with an air mass (AM 1.5 spectrum).

The parameters and equations of the circuit model presented in this section depend on the STC. I_{PV} which depends exponentially on solar irradiance and is impacted by changes in temperature and irradiance, it can be corrected by (5):

$$I_{PV} = (I_{PV,STC} + K_I \Delta T) \frac{G}{G_{STC}} \tag{5}$$

G is the amount of irradiance that is present on the surface of the cell, and G_{STC} refers to 1000 W/m$^{2.}$ K_I represent the current's temperature coefficient, the difference in temperature between the cell and the standard 25°C is denoted by ΔT. Another interesting fact about diodes is that they have a reverse saturation current (I_0) that is greatly influenced by temperature, and it can be modelled by (6)[37]:

$$I_O = \frac{I_{SC,STC} + K_I \Delta T}{exp \left[\frac{q(V_{OC,STC} + K_V \Delta T)}{nKT} \right] - 1} \tag{6}$$

Short circuit current and open circuit voltage are characterized by $I_{OC,STC}$ and $V_{SC,STC}$ correspondingly, whereas temperature coefficients for current and voltage are denoted by the K_I and K_V, respectively. The normal operating cell temperature (NOCT) parameters given in the datasheets are commonly used to determine T_{cell} of the solar cell. Open circuit cells with 800 W/m^2, a temperature of 20°C and a wind speed of 1 m/s attain a temperature known as NOCT. As a result, T_{cell} may be computed from NOCT using this method (7):

$$T_{cell} = T_a + \frac{G}{800} (NOCT - 20) \tag{7}$$

2.3. PSCs and bypass diodes effects

A PV module is generally made up of solar cells that are linked in series and/or parallel to produce the required output voltage. Consequently, (1) can be modified to describe the current of a PV module and shown in the form of (8):

$$I = N_P I_{PV} - I_O \left\{ exp \left[\frac{q(V + IR_S)}{nKTN_S} \right] - 1 \right\} - \frac{V + IR_S}{R_P} \tag{8}$$

N_S stands for the number of cells that are linked in series; N_p stands for the number of cells that are linked in parallel. In the same way, PV arrays comprise of a group of interconnected PV modules, and PV modules are often protected from reverse flow and hot spots using blocking and bypass diodes. At the same time, the P–V curve under PSCs may display several LMPPs if bypass diodes are included in the circuit. The tracking of MPP becomes more difficult as a result of this [38].

Figure 2 shows a PV string where, PV modules linked in series with blocking and bypass diodes. Each module in the string is joined with a bypass diode to avoid overheating. Furthermore, each string of PV modules is ended with a blocking diode. When measuring the voltage drop over the blocking diode V_{bl} and the voltage across individual PV module V_{md}, the whole voltage across the PV string V_{st} can be computed by adding the previous two values together. It is also important to note that each module's string short circuit current I_{SCi} (nearly equivalent to the module photocurrent) and string current I_{st} are used to compute $V_{md,i}$. It is possible to compute $V_{md,i}$ through using the Lambert W function if I_{st} is equal to or lower than I_{SCi}; however, if I_{st} is more than I_{SCi}, this allows the bypass diode to conduct, and the $V_{md,i}$ is clamped at a tiny voltage which is similar to diode's forward bias voltage. This means that the bypass diode is responsible for carrying the discrepancy between the I_{st} and I_{SCi}. A mathematical model of how PV string voltage V_{st} and current I_{st} are related can be described as follow:

$$V_{ST} = \sum_{i=1} V_{md,i} + V_{bl} \tag{9}$$

$$V_{md,i} \begin{cases} R_P \times (I_{PV} + I_O) - (R_S + R_P) \times I_{ST} - a \times W \\ \left\{ \frac{R_P I_O}{a} exp \left[\frac{R_P(I_{PV} + I_O - I_{ST})}{a} \right] \right\}, I_{ST} \leq I_{SC,i} \\ -\frac{n_{bp} KT}{q} \times ln \left(\frac{I_{ST} - I_{SC,i}}{I_{O,bp}} + 1 \right), I_{ST} > I_{SC,i} \end{cases} \tag{10}$$

$$V_{bl} = -\frac{n_{bl} KT}{q} \times ln \left(\frac{I_{ST}}{I_{O,bl}} + 1 \right) \tag{11}$$

Where $I_{O,bl}$ refers to the blocked diode's reverse saturation currents, whereas $I_{O,bp}$ refers to the bypass diode's reverse saturation currents, $W(x)$ indicates the Lambert W function diodes, n_{bp} refers to the bypass diodes ideality constant, whereas n_{bl} refers to the blocking diodes ideality constant.

It is possible that the value of $I_{SC,i}$ in (10), will be variable for each of the modules that comprise a PV string when using PSCs. Because of this, the I–V curves could have steps, and the P–V curves might have several LMPP. A PV array is seen in Figure 3 under the conditions of uniform irradiance (Pattern A) and PSC (Pattern B). The PV array includes four PV modules that are coupled in series. Figure 4 depicts the results of a series connection of four modules, each of which
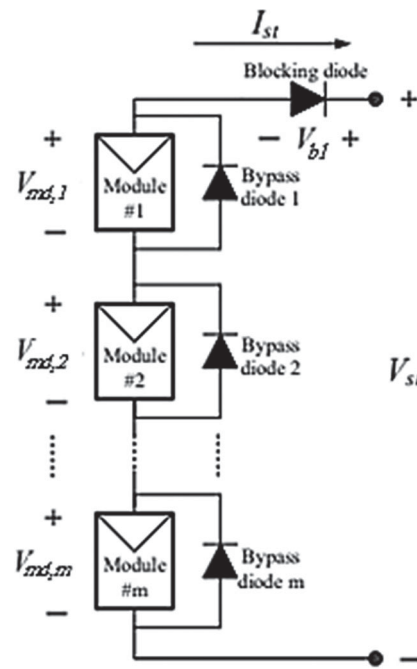

Figure 2. Shows a PV string that includes blocking and bypass diodes.

is exposed to a different level of irradiance, the P–V curves have an LMPP number of 4, and the interval number is also 4. Because of this, the P–V curve that is produced will be more complex, producing several peaks in a single array along with extended strings. When this occurs, standard MPPT algorithms might get stuck at one LMPPs and miss the GMPP entirely, which can cause the PV modules' output power to be drastically reduced. Additionally, there is a high probability that the irradiance level will vary quickly, leading to shifts in the GMPP's position. In light of this, the MPPT algorithm has to rapidly and precisely identify the GMPP among the LMPPs to capture the highest power that the PV system generates while subject to PSCs.

3. Overview of Grey wolf optimization

According to Mirjalili et al. [39], the GWO algorithm was developed to mimic the social hierarchy and hunting strategies of grey wolves in their native environment. Predators, such as grey wolves, prefer to travel in social groups known as packs rather than alone. Grey wolves of the alpha (α), beta (β), delta (δ) and omega (ω) species are used to represent the several levels of hierarchy. In addition, they maintain a very rigid social dominant hierarchy, which can be seen in Figure 5, where the level of dominance held by each wolf decreases as one moves down the hierarchy. At GWO, the alpha (α) mathematically represents the fittest solution to model the wolf social hierarchy. The best solutions that came in second and third place, respectively, have been labelled with the beta (β), delta
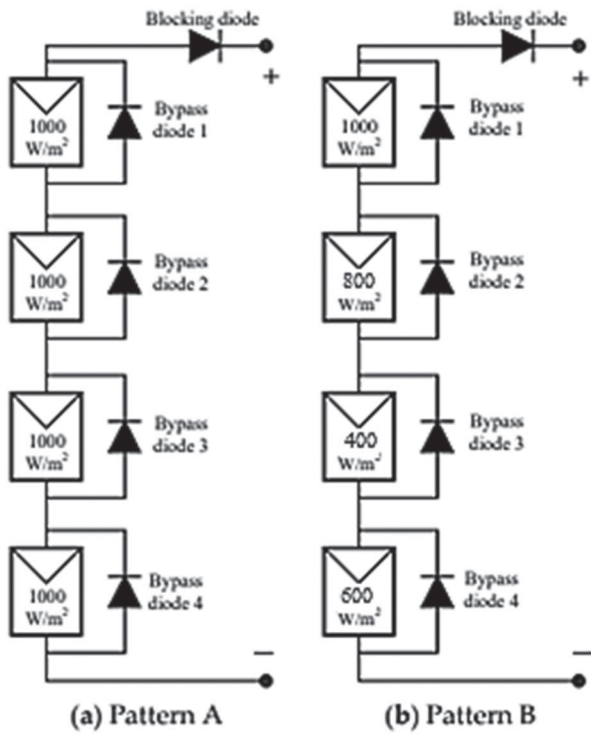
Figure 3. PV array function under (a) uniform irradiance (b) partial shading condition (PSC).

(δ). All other solutions are assumed to be omega (ω). The GWO engages in primary processes, which are displayed in Figure 6: hunting, chasing and tracking for prey; encircling prey and attacking prey. During the hunt, wolf packs circle their prey. The following equations can model this behaviour.

Grey wolf positions may be updated using the (12) and (13) [35]:

$$\vec{D} = |\vec{C} \times \vec{X}_P(t) - \vec{X}(t)| \qquad (12)$$

$$\vec{X}(t+1) = \vec{X}_P(t) - \vec{A} \times \vec{D} \qquad (13)$$

where t denotes the current iteration, X_P represents the prey position, the grey wolf's position is indicated by the X. A, C and D represent the coefficient vectors. Vectors A and C can be determined as follows [16]:

$$\vec{A} = 2\vec{a} \times \vec{r}_1 - \vec{a} \qquad (14)$$

$$\vec{C} = 2 \times \vec{r}_2 \qquad (15)$$

The random variables r_1 and r_2 are in the range [0,1], and their values drop gradually from 2 to 0. Hunting is generally directed by α in their search (optimization). The β and δ may hunt on occasion. These three wolves are being pursued by the other wolves. The following formula should be used while updating position:

The grey wolves will begin their attack as soon as their prey stops moving.

$$\vec{D}_\alpha = |\vec{C}_1 \times \vec{X}_\alpha(t) - \vec{X}(t)|,$$
$$\vec{D}_\beta = |\vec{C}_2 \times \vec{X}_\beta(t) - \vec{X}(t)|,$$

$$\vec{D}_\delta = |\vec{C}_3 \times \vec{X}_\delta(t) - \vec{X}(t)| \qquad (16)$$

$$\vec{X}_1 = \vec{X}_\alpha(t) - \vec{A}_1 \times \vec{D}_\alpha,$$
$$\vec{X}_2 = \vec{X}_\beta(t) - \vec{A}_2 \times \vec{D}_\beta,$$
$$\vec{X}_3 = \vec{X}_\delta(t) - \vec{A}_3 \times \vec{D}_\delta \qquad (17)$$

$$\vec{X}(t+1) = \frac{\vec{X}_1 + \vec{X}_2 + \vec{X}_3}{3} \qquad (18)$$

## 4. The novel GWO algorithm and its use in MPPT design

4.1. Novel Grey wolf optimization (NGWO)

In this proposed method, Grey Wolf Optimization (GWO) is integrated with the Cuckoo Search (CS) abandoning mechanism to minimize the time spent on tracking. The unique brooding behaviour of cuckoos drives CS: cuckoos lay their eggs in the nests of host bird species to enhance their offspring's chances of survival. However, there is a risk that the cuckoo's eggs will be discovered by the host, who may then destroy or abandon them. This approach has been combined with BA to improve the tracking performance of the BA [40] The implementation of CS is guided by three idealized principles:

- The nests in which cuckoos deposit their eggs are chosen randomly.
- Only the highest quality eggs are retained for the next generation.
- A predefined number of host nests exist, and the probability that the host will detect foreign eggs is represented by P_a [0, 1]. If the host discovers alien eggs, it will destroy the nest or abandon it and build a new one elsewhere. This can be simulated by replacing a percentage P_a of N nests with new solutions. The inclusion of the CS abandoning mechanism restricts the search to potentially feasible candidate solutions, potentially speeding up convergence. It is recommended to integrate the abandonment concept into GWO to enhance convergence speed. Before activating the abandonment mechanism, the positions of the grey wolves X_i are sorted in ascending order, and the poorest performers are replaced with new entries. Ultimately, a number of N_r grey wolves are abandoned. The difference between the abandoned grey wolf position X_{ab} and the global best position X_{bes} can be determined by (19). This ensures an equivalent number of grey wolves are replenished.

$$\Delta X_{ab} = |X_{best} - X_{ab}| \qquad (19)$$

A comparison will be made between the value of ΔX_{ab} and a threshold value of Thr. It can be deduced that the worst grey wolf X_{ab} is very close to X_{best} if the value of ΔX_{ab} is either equal to or smaller than Thr. As
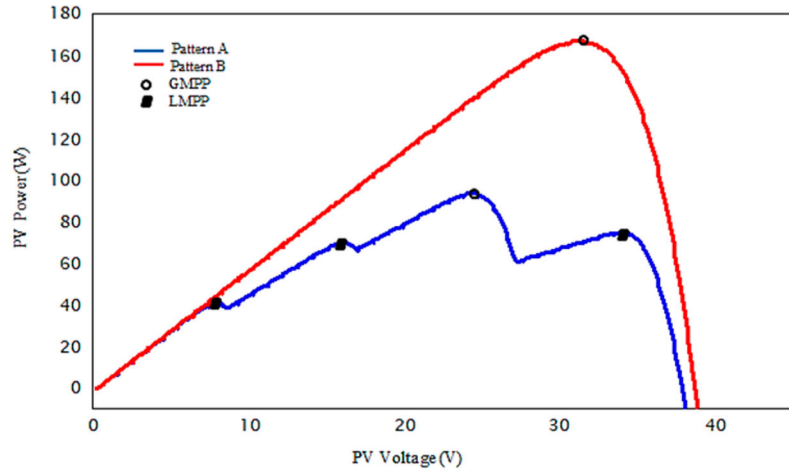
(a)
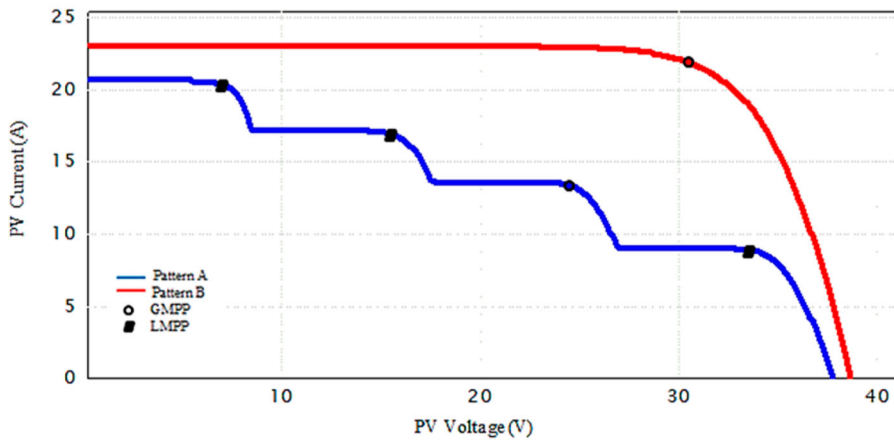
(b)

Figure 4. Shows (a) P–V curve under normal irradiance and PSC (b) I–V curve under normal irradiance and PSCs.
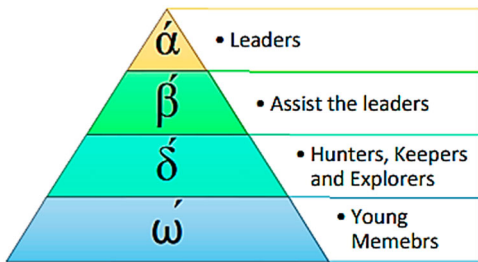

Figure 5. The grey wolf's hierarchical order.

a result, the value of the regenerating grey wolf, $X_{i,new}$, has been set to X_{best}. Nevertheless, if the value of ΔX_{ab} is more than *Thr*, this indicates that X_{ab} is a considerable distance from X_{best}. As a result, the regenerating grey wolf can be described based on the form of (20).

$$X_{i,new} = X_{best} \pm \Delta R_i \qquad (20)$$

Then ΔR_i can be defined in (21):

$$\Delta R_i = r \times \Delta X_{ab} \times F_c \qquad (21)$$

where r is a random number between 0 and 1, and the following expression describes the cooling factor F_c:

$$F_c = \frac{1}{t} \qquad (22)$$

Consideration is given to the following factors when deciding whether ΔR_i should be added or subtracted from X_{best} Suppose that X_{cb} is the current iteration's best solution. To put it another way if $X_{best} > X_{cb}$, it means that X_{cb} is to the left of X_{best}. Thus, the regenerating grey wolf $X_{i,new}$ is set as the corresponding Equation (23) to discover the left side of X_{best}, as can be seen in Figure 7(a).

$$X_{i,new} = X_{best} - \Delta R_i \qquad (23)$$

Figure 7(b) shows the changes in the search space as shown in this scenario. The search space includes zones 1 and 2. This can conceivably speed up the convergence time of the system by removing X_2 (X_{ab}) from the left subspace in Figure 7(b) and putting the regenerating grey wolf $X_{2,new}$; in this case, the search space excludes zone 1 and retains only zone 2. However, X_{cb}
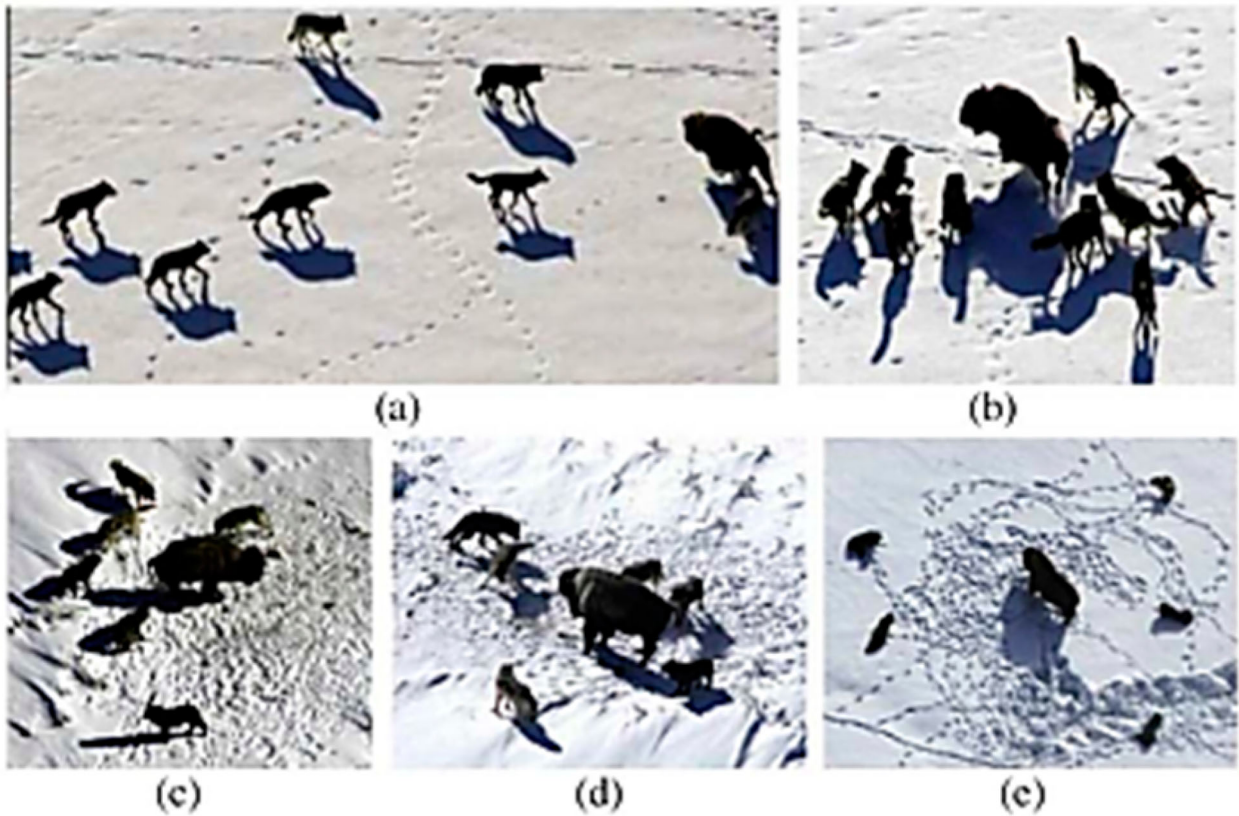
Figure 6. Grey wolf hunting strategies: (a–c) following, and tracking prey (d) encircling (e) stationary situation and attack.

is set on the right side of the X_{best} when the $X_{best} < X_{cb}$. Figure 8(a) shows how to explore the right side of X_{best} by setting $X_{i,new}$ as (24).

$$X_{i,new} = X_{best} + \Delta R_i \qquad (24)$$

Figure 8(b) depicts how the search space changes in this scenario by removing X_2 (X_{ab}) and replacing it with $X_{2,new}$ as per (24), all of the wolfs are restricted to the right subspace (Zone 2).

4.2. The implementation of a novel GWO for the purpose of MPP tracking

Figure 9 shows the flowchart of NGWO-based MPPT algorithm. V_{pv} and I_{pv} are measured by sensors and the output power is determined for a given number of grey wolves, or duty cycles.

The P–V curve contains a number of peaks as a consequence of the condition of partial shading that took place, each with LMPPs and a one GMPP. As it turns out, when wolves locate the GMPP, their associated coefficient vectors almost reach zero. This method attempts to incorporate the proposed NGWO control and maintain of the duty cycle constantly at the MPP; this could diminishes the steady-state oscillations that are characteristic of classic MPPT approaches, which, in turn, minimizes the power loss that is occurred by oscillation, which ultimately increases in the system's overall efficiency. When using an MPPT built upon the NGWO, the duty cycle D is referred to as a grey wolf.

As a consequence of this, (16)–(18) are modified in the ways that are described in the following:

$$\vec{D}_\alpha = |\vec{C}_1 \times \vec{d}_\alpha(t) - \vec{d}(t)|,$$
$$\vec{D}_\beta = |\vec{C}_2 \times \vec{d}_\beta(t) - \vec{d}(t)|,$$
$$\vec{D}_\delta = |\vec{C}_3 \times \vec{d}_\delta(t) - \vec{d}(t)| \qquad (25)$$
$$\vec{d}_1 = \vec{d}_\alpha(t) - \vec{A}_1 \times \vec{D}_\alpha, \vec{d}_2 = \vec{d}_\beta(t) - \vec{A}_2 \times \vec{D}_\beta,$$
$$\vec{d}_3 = \vec{d}_\delta(t) - \vec{A}_3 \times \vec{D}_\delta \qquad (26)$$
$$\vec{d}(t+1) = \frac{\vec{d}_1 + \vec{d}_2 + \vec{d}_3}{3} \qquad (27)$$

where D_α and D_β are the distances of d_α and d_β from the point where the power is at its maximum.

This leads to the following formulation for the fitness function of the GWO algorithm:

$$P(d_i^k) > P(d_i^{k-1}) \qquad (28)$$

where d stands for the duty cycle, P stands for output power, i represents the grey wolf's number, and the number of iterations is denoted by k.

The proposed NGWO includes the following steps:

Step 1: Initialization of the parameters: The first step is to set up the parameters. To begin, a four-duty cycle with a range of [0, 1] is generated. During the GMPP exploration phase, particles are initiated on the left, Centre, and right sides to guarantee that every search
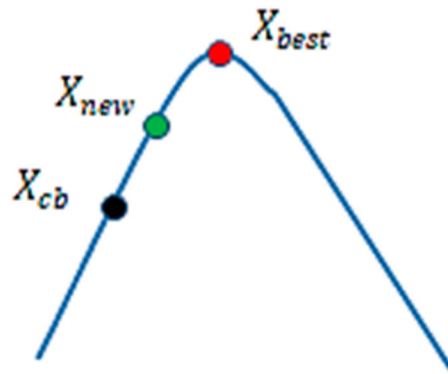
(a)
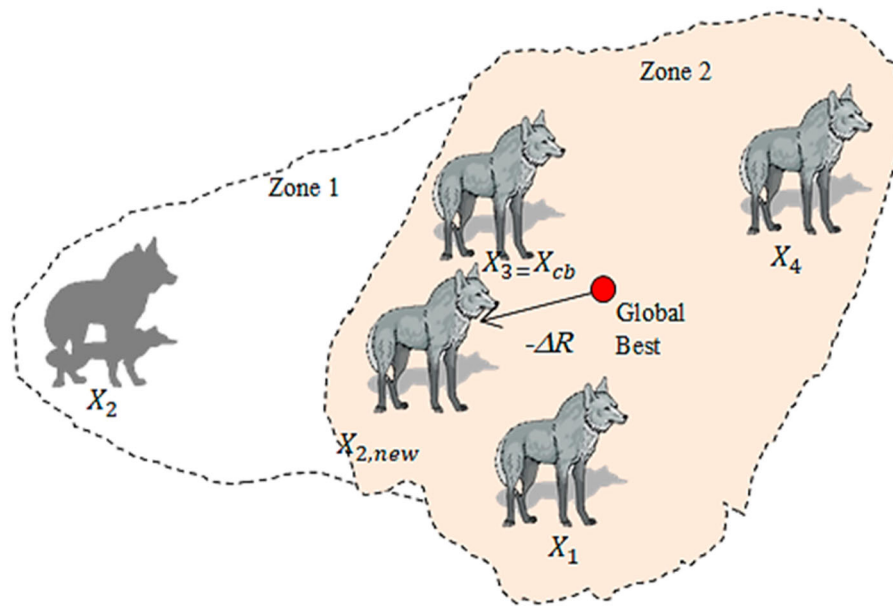
(b)

Figure 7. (a) The case when $X_{best} > X_{cb}$ (b) After sorting by fitness, Grey wolf positions include Zones 1 and 2 of the search space. (b) The abandonment mechanism reduced the search space to only zone 2.

space is completely covered. These calculations, the starting positions are as follows: (0.1, 0.4, 0.6 and 0.9).

Step 2: Evaluation of fitness: includes the subsequent computation of the PV array's output power corresponding to each duty cycle. Current and voltage measurements are required for this purpose. In terms of fitness, the duty cycle, which is regarded as the optimal solution maps to the maximum possible power level donated by $D_{i,best}$. In terms of fitness, the duty cycle, which is regarded as the worst solution maps to the minimum possible power level donated by $D_{i,worst}$.

Step 3: See whether $rand > p_a$. If this is the case, proceed to Step 4; else, go to Step 6.

Step 4: Replace the worst grey wolves (duty cycles) with new ones using the abandoning mechanism

using (19)–(24), then see whether $d_i^{kworst} > d_{max}$, then $d_i^{kworst} = d_{max}$; alternatively, if $d_i^{kworst} < d_{min}$, then $d_i^{kworst} = d_{min}$.

Step 5: Send the new worst value d_i^{kworst} to the PV system so that it can compute the P_i^{kworst}, then check if $P_i^{kworst} > P_{max}$, then $P_{max} = P_i^{kworst}$, $d_{max} = d_i^{kworst}$; otherwise keep the previous value of P_{max} and d_{max}

Step 6: Update the position of grey wolfs (duty cycles) using an equation of GWO (25)–(27), then check if $d_i^{kworst} > d_{max}$, then $d_i^{kworst} = d_{max}$; otherwise, if $d_i^{kworst} < d_{min}$, then $d_i^{kworst} = d_{min}$.

Step 7: Send the new value of worst d_i^k to the PV system so that it can compute the P_i^k, then check if $P_i^{kt} > P_{max}$, then $P_{max} = P_i^k$, $d_{max} = d_i^k$; otherwise keep the previous value of P_{max} and d_{max}
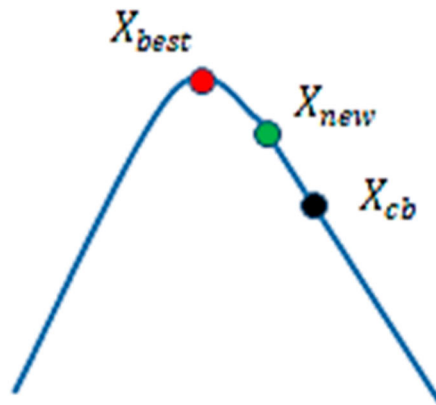
(a)
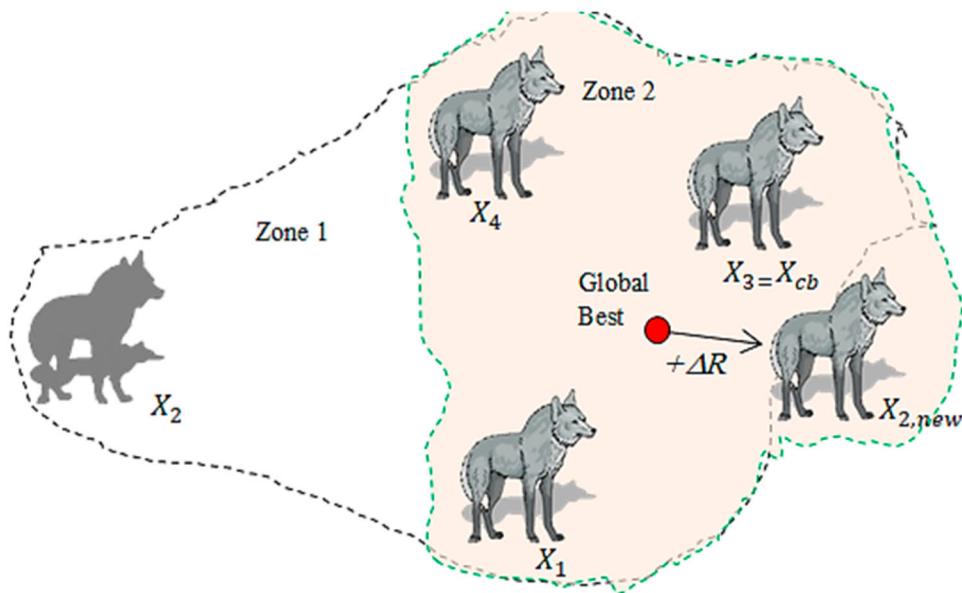
(b)

Figure 8. (a) The case when $X_{best} < X_{cb}$ Figure 5 (b) After sorting by fitness, Grey wolf positions include Zones 1 of the search space. (b) The abandonment mechanism reduced the search space to only zone 2.

Step 8: Checking the iteration there is an evaluation of the convergence criterion. The calculation will be finished when the predetermined iteration number has been attained. If this is not the case, it is expected that steps 2 through 7 will be repeated until the termination requirements are met.

Step 9: The change in the environment may affects the maximum output power of a PV system. The proposed NGWO algorithm uses a restart mechanism to respond quickly to changes in PSC. For the proposed

NGWO algorithm to restart, the following equation must be valid: Evaluate the stopping criteria shown in (29). Proceed to Step 1 if it is valid; otherwise, continue to Step 2.

$$\frac{P_i - P_m}{Pm} > \Delta P \qquad (29)$$

Where P_i is the new actual output power, P_m is the output power of the PV array measured at MPP depending on the conditions of the most current operation, and the
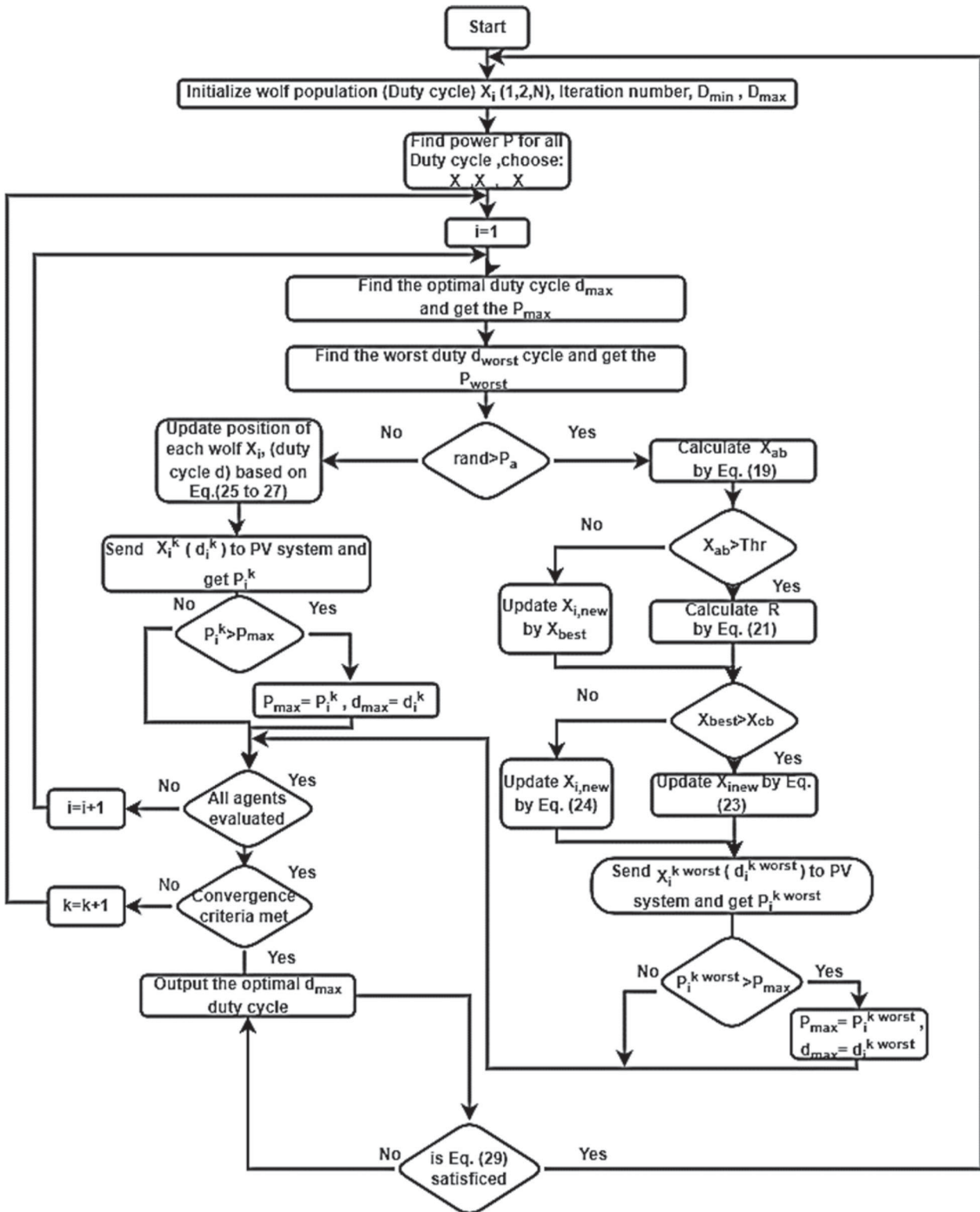
Figure 9. Flowchart of the proposed NGWO algorithm.

PV array's output power change threshold is denoted by ΔP.

5. Simulation analysis and discussion

A simulation study in MATLAB/SIMULINK was conducted to verify the effectiveness of the proposed NGWO method. Figure 10 illustrates the basic structure of the PV system explored in this study, which consists of a PV array, a battery pack, a DC-DC boost converter, and an MPPT controller. The converter was designed to operate in continuous inductor current mode. The key properties of the PV module are presented in Table 1.

Four PSC patterns are used to assess the algorithm's effectiveness: patterns (Figure 11), which are generated sequentially by varying the irradiation levels of the four modules (0.9, 1, 0.85, 0.5) [kW/m²], (0.9, 0.6, 0.5, 1)
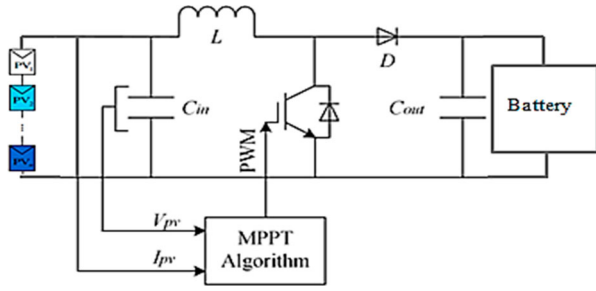
Figure 10. Block diagram of the proposed PV system.

Table 1. PV module specification.

Specification of single PV module	Values
Maximum Power (P_{mpp})	41.05 W
Open Circuit Voltage (V_{oc})	9.87 V
Maximum Power Voltage (V_{mpp})	7.41 V
Short Circuit Current (I_{SC})	5.76 A
Maximum Power Current (I_{MPP})	5.54 A
Configuration of PV module	4-Series

Table 2. Parameter sets for various MPPT algorithms.

Algorithms	Parameters
P&O	$\Delta d = 0.01$, d = 0.6
GWO	a from 2 to 0 and r_1 and $r_2 = \{0,1\}$
EGWO	a – self-adaption
NGWO	$P_a = 0.25$, a from 2 to 0 and r_1 and $r_2 = \{0,1\}$,

[kW/m^2], (0.9, 0.9, 0.5, 0.9) [kW/m^2], and (0.7, 0.8, 0.8, 1) [kW/m^2] (Table 2).

Two alternative soft computing algorithms, the Grey Wolf Optimization (GWO) algorithm proposed in [35] and the conventional Perturb & Observe (P&O) algorithm, were compared with the NGWO to verify the reliability of the proposed NGWO algorithm. Each algorithm was evaluated using the same model and under identical conditions. Power, current and voltage waveforms, along with their overall performance, are displayed for each method in Figures 12–15. Both NGWO and the other soft computing methods successfully detected the GMPP as shown in the figures. However, they differed in tracking speed, oscillation around the GMPP, and efficiency; notably, the P&O algorithm tends to get trapped at the Local Maximum Power Point (LMPP) rather than the GMPP. Table 3 lists the numerical results for each algorithm, with the NGWO outperforming all compared methods. In the simulation, voltage and current values are recorded using oscilloscope readings. The voltage measurement, denoted as V_m, typically has an uncertainty, ΔV_m, of ±0.1 V, while the current measurement, I_m, carries an uncertainty, ΔI_m, of ±5 mA. The uncertainty in power measurement, ΔP_m, can be calculated as follows:

$$\Delta P_m \cong V_m \Delta I_m + I_m \Delta V_m \tag{30}$$

In this study, the usual uncertainty or sensitivity in power measurement ranges from ±0.3 to ±0.7 W.

The first simulation study (Section 5.1) demonstrates how well the proposed method functions for various shading patterns. The second simulation study (Section 5.2) will analyse each optimization method using a range of peak numbers and swarm sizes to determine its effectiveness. The following provides further information regarding these two studies.

5.1. The statistical performance of NGWO under PSC

In pattern (1): As shown in Figure 11(a), the GMPP is located at the centre of the P–V curve at 111.87 W. Figure 12 presents the simulation results for several algorithms under pattern 1. The GWO algorithm reaches the GMPP in 0.48 s with a GMPPT efficiency of 99.50%. In contrast, EGWO [35] tracks the GMPP in only 0.36 s with a GMPPT efficiency of 99.62%. Although the P&O algorithm can operate rapidly in 0.16 s, it fails to track the GMPP and instead captures one of the local LMPPs, resulting in a tracking efficiency of 85.45%. However, the proposed NGWO algorithm takes only 0.22 s with a tracking efficiency exceeding 99.90%, indicating that NGWO's tracking time is about 63% and 113% quicker than the EGWO and GWO algorithms, respectively.

In pattern (2): As shown in Figure 11(b), the GMPP is on the right side of the P–V curve at 93.8 W, and all algorithms were able to detect it. Figure 13 displays the simulation results for several algorithms under pattern 2. It takes 0.41 s for the GWO-based MPPT to stabilize at the GMPP, with a tracking efficiency of 99.58%. Meanwhile, EGWO [35] tracks the GMPP in 0.37 s with a tracking efficiency of 99.48%. The P&O algorithm also effectively converges to the GMPP, achieving a tracking efficiency of 99.42%. GWO similarly tracks the GMPP with a tracking efficiency of 99.42%. Additionally, the P&O algorithm's ability to detect GMPP is influenced by the search starting location. The P&O approach, for example, cannot track the GMPP if the beginning point for a search is a duty cycle of 0.2 s. However, the proposed NGWO method takes 0.17s to attain the GMPP and has a tracking efficiency of 99.72%.

In pattern (3): As shown in Figure 11(c), the GMPP is located on the left side of the P–V curve at 112.81 W. Figure 14 presents the simulation results for several algorithms under pattern 3. Although the P&O algorithm only requires 0.18 s to track an MPP, it erroneously tracks the LMPP instead of the GMPP, resulting in significantly lower MPPT efficiency due to getting stuck at the LMPP. In scenarios where the output powers were 112.66, 112.69 and 112.72 W, respectively, the GWO, EGWO [35], and the proposed NGWO algorithms took 0.48, 0.39 and 0.17 s to track the GMPP. The tracking efficiency of the four algorithms ranged from 87.16% to 99.86%, 99.89% and 99.92%, respectively. Consequently, the NGWO algorithm proves to be quicker and more efficient than the other MPPT algorithms. Additionally, the proposed NGWO exhibits
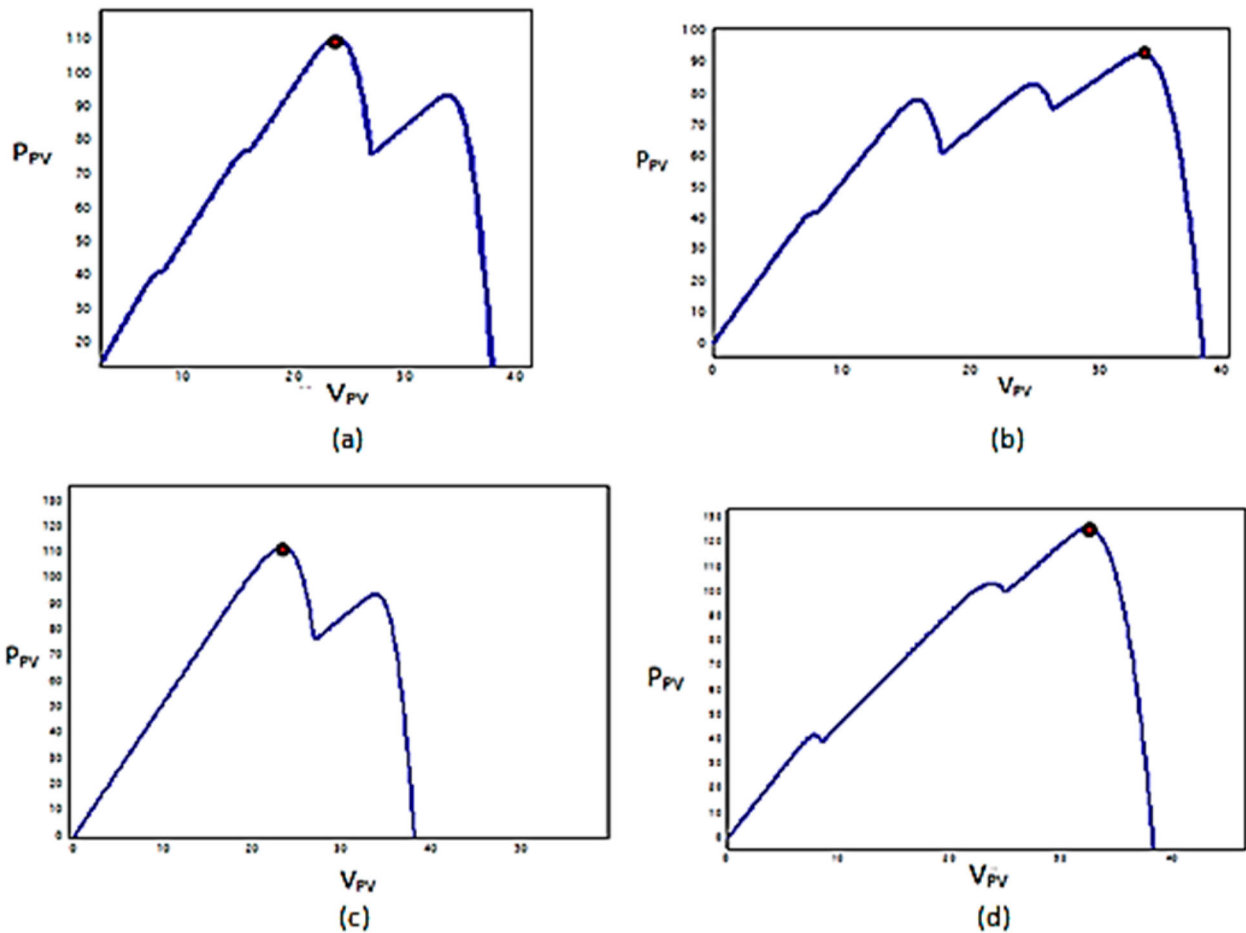
Figure 11. Different PSC layouts for PV arrays that have been adopted.

Table 3. Comparison analysis of the GWO, EGWO, NGWO and *P*&O algorithms under four different patterns.

Cases	Index	P&O	GWO	EGWO[35]	NGWO
Case 1 Rated Power (W) = 111.87 W	P_{mpp}	95.6W	111.31W	111.45W	111.76W
	T(s)	0.16	0.48	0.36	0.22
	η	85.45%	99.50%	99.62%	99.90%
Case 2 Rated Power (W) = 93.8 W	P_{mpp}	93.26W	93.40W	93.48W	93.54W
	T(s)	0.19	0.41	0.37	0.17
	η	99.42%	99.58%	99.65%	99.72%
Case 3 Rated Power (W) = 112.81 W	P_{mpp}	95.33W	112.66W	112.69W	112.72W
	T(s)	0.18	0.48	0.39s	0.17s
	η	84.50%	99.86%	99.89%	99.92%
Case 4 Rated Power (W) = 126.80 W	P_{mpp}	125.29W	126.4W	126.54W	126.66W
	T(s)	0.18	0.39	0.37	0.21
	η	98.80%	99.68%	99.79%	99.89%

noticeably fewer oscillations compared to other MPPT algorithms. Figure 15 will show the simulation results under pattern 4.

According to the data summarized in Table 3, the solutions obtained from the proposed NGWO are almost always located at the global optima, indicating that additional energy is attained. Furthermore, the NGWO exhibits the highest level of efficiency, averaging 99.86%. NGWO outperforms the other MPPT algorithms in terms of performance. The GMPP takes an average of 0.19 s to track using NGWO, but the GWO and EGWO take 0.44 and 0.38 s, respectively. Simulation results show that NGWO outperforms the compared methods in every performance criteria.

5.2. NGWO performance under PSC in a dynamic environment

The NGWO-based GMPPT approach is further validated by employing a changing sequence of Patterns 1 – Pattern 2 – Pattern 3 – Pattern 4 to observe changes in the curve and verify the simulation. A re-initialization strategy was implemented to ensure the MPPT algorithm functions properly despite constantly changing irradiance levels, which shift after exactly one second. Figure 16 displays the results of each algorithm's simulation, including GWO, EGWO, NGWO and P&O, showing the waveform of the PV output power, voltage and current. The simulation starts with the PV array operating according to Pattern 1. The
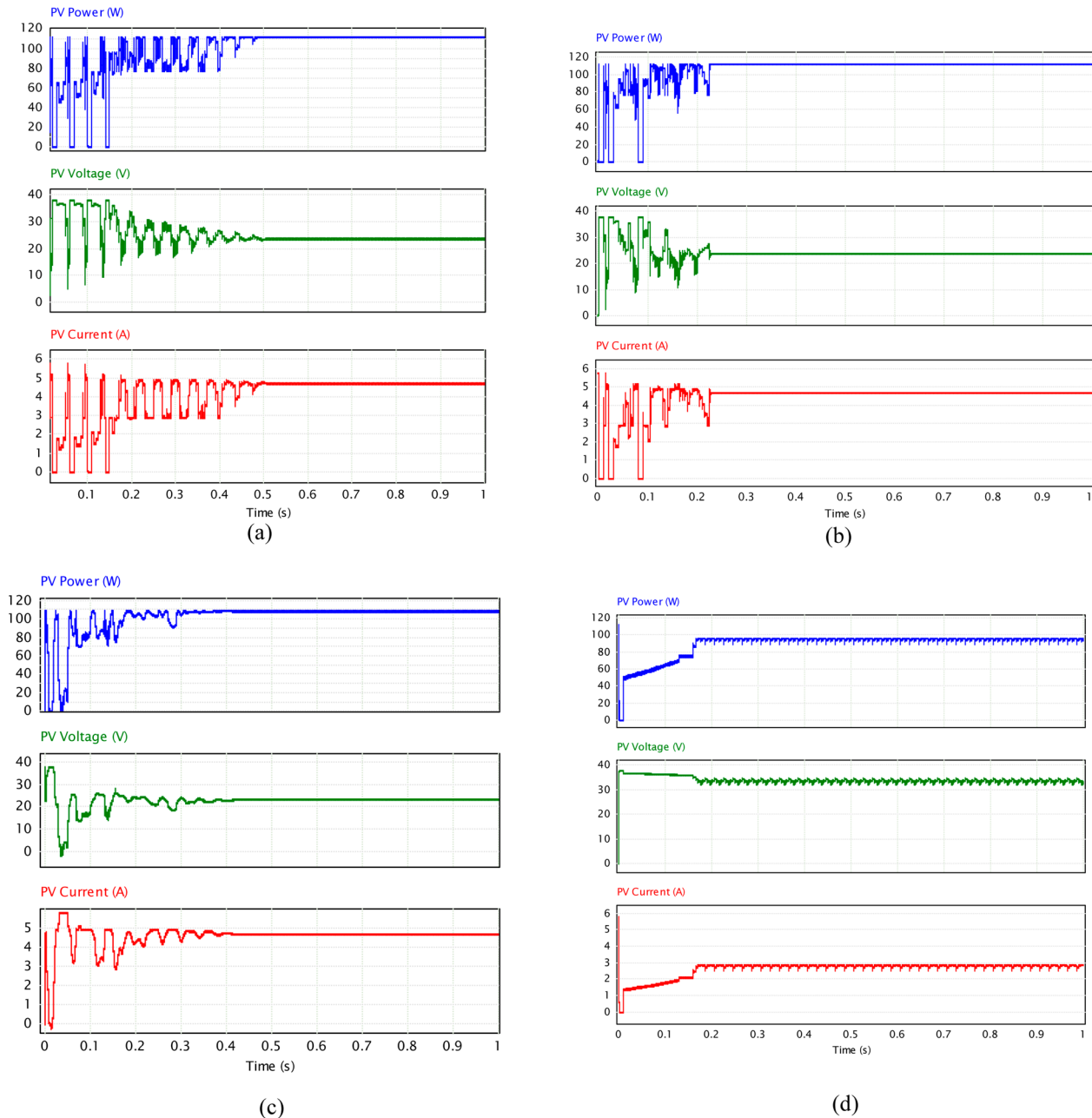
Figure 12. PV array output voltage, current and power waveforms for pattern 1: (a) GWO, (b) EGWO [35], (c) NGWO and (d) P&O.

EGWO MPPT algorithm requires approximately 0.22 s to track the GMPP. At the time t = 1 s, the irradiance of the PV array has altered, which ultimately results in the irradiance moving to pattern 2. The change is recognized by the algorithm under consideration, which then restarts its tracking of the new GMPP. The new GMPP is tracked by the NGWO algorithm in about 0.17 s when pattern 2 is used. The simulations' results reveal that the NGWO demonstrates a good dynamic performance. Once the time t = 2 s has passed, the PV array's irradiance shifts to pattern 3. The new GMPP is tracked by the proposed NGWO, which identifies the change and restarts the tracking process. Tracking the new GMPP under pattern 3 takes roughly 0.17 s. As time goes on, the PV array is exposed to different solar radiation patterns, which occur at t = 3 s. The

NGWO algorithm tracks the new GMPP, identifying the change and restarting the tracking process. The NGWO algorithm takes roughly 0.21 s to track the new GMPP under pattern 4.

Table 4 presents a comparison of the proposed method with existing MPPT techniques. The results conclusively demonstrate that the proposed method is more reliable, accurate and faster, making it a superior option for identifying the GMPP of the PV system under various partial shading conditions.

The optimization methods were studied under three different partial shading conditions (PSC) with one, five and ten peaks, using 4, 6, 8 and 10 searching agents or swarm-size values. The findings, which include convergence time and failure rate (FR), are presented in Table 5. Swarm optimization
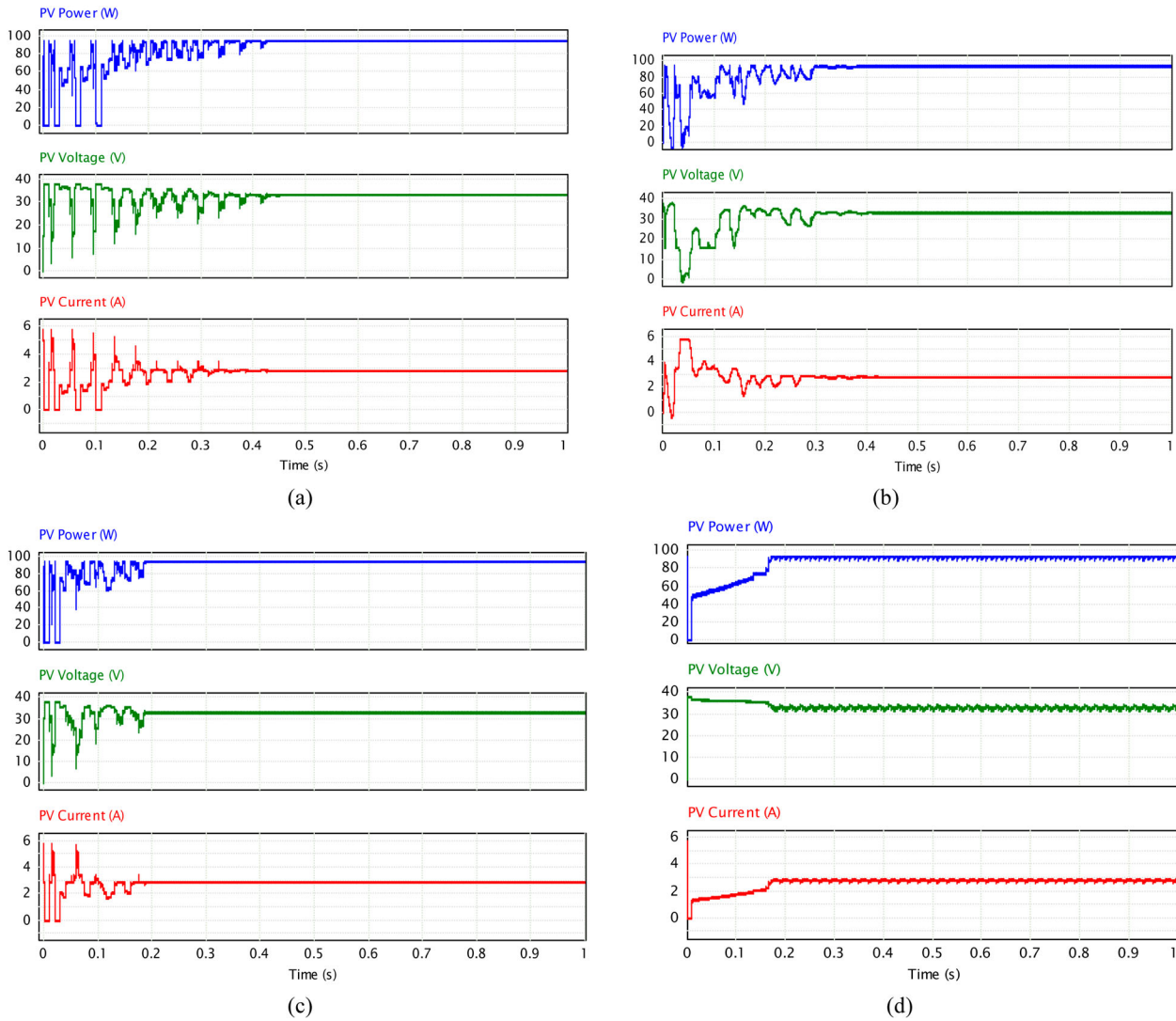
Figure 13. PV array output voltage, current and power waveforms for pattern 2: (a) GWO, (b) EGWO [35], (c) NGWO and (d) P&O.

Table 4. Comparative analysis of the performance of the proposed method against other MPPT approaches in the literature.

Parameters	P&O [7]	PSO [11]	ABC [22]	ACO [23]	GWO [27]	EGWO [35]	Proposed method
Complexity	Low	Moderate	Moderate	Moderate	High	Moderate	Moderate
Efficiency	Low (under PSC)	Moderate	Moderate	Moderate	High	High	Very High
Tracking capability of GMPP	Low	High	Moderate	High	High	High	High
Tracking speed	High	Moderate	High	Moderate	High	High	Very High
Steady-state oscillation	Yes	No	No	No	No	No	No

strategies performed admirably in scenarios with a single peak.

In comparison, the proposed NGWO method demonstrated its superiority by acquiring the GMPP in less than half the time required by GWO, with respective times of 0.15, 0.19, 0.31, 0.44 and 0.49 s for 3, 4, 6, 8 and 10 searching agents. When facing 5 peaks with three searching agents, GWO took 0.41 s to find the GMPP and had a failure rate of 14%. In contrast, NGWO tracked the GMPP in just 0.18 s with a failure rate of 11%, while EGWO took 0.32 s with a failure rate of 15%. It is essential to note that the low number of agents is directly linked to the high failure rate. With four searching agents, NGWO quickly acquired the GMPP with a 0% failure rate, significantly outperforming other optimization methods, which demonstrated longer convergence times and higher failure rates. With six searching agents, no optimization methods recorded any failure rate. The time it took for NGWO to capture the GMPP was 0.38 s, compared to 0.57 and 0.53 s for GWO and EGWO, respectively. When the number of searching agents increased to 8 or 10, the failure rate remained at 0% for all optimization methods, but the time to converge towards the GMPP increased; NGWO still had the quickest convergence time. For P–V curves containing five peaks or fewer, it is advisable to use at least four searching agents with the NGWO algorithm.
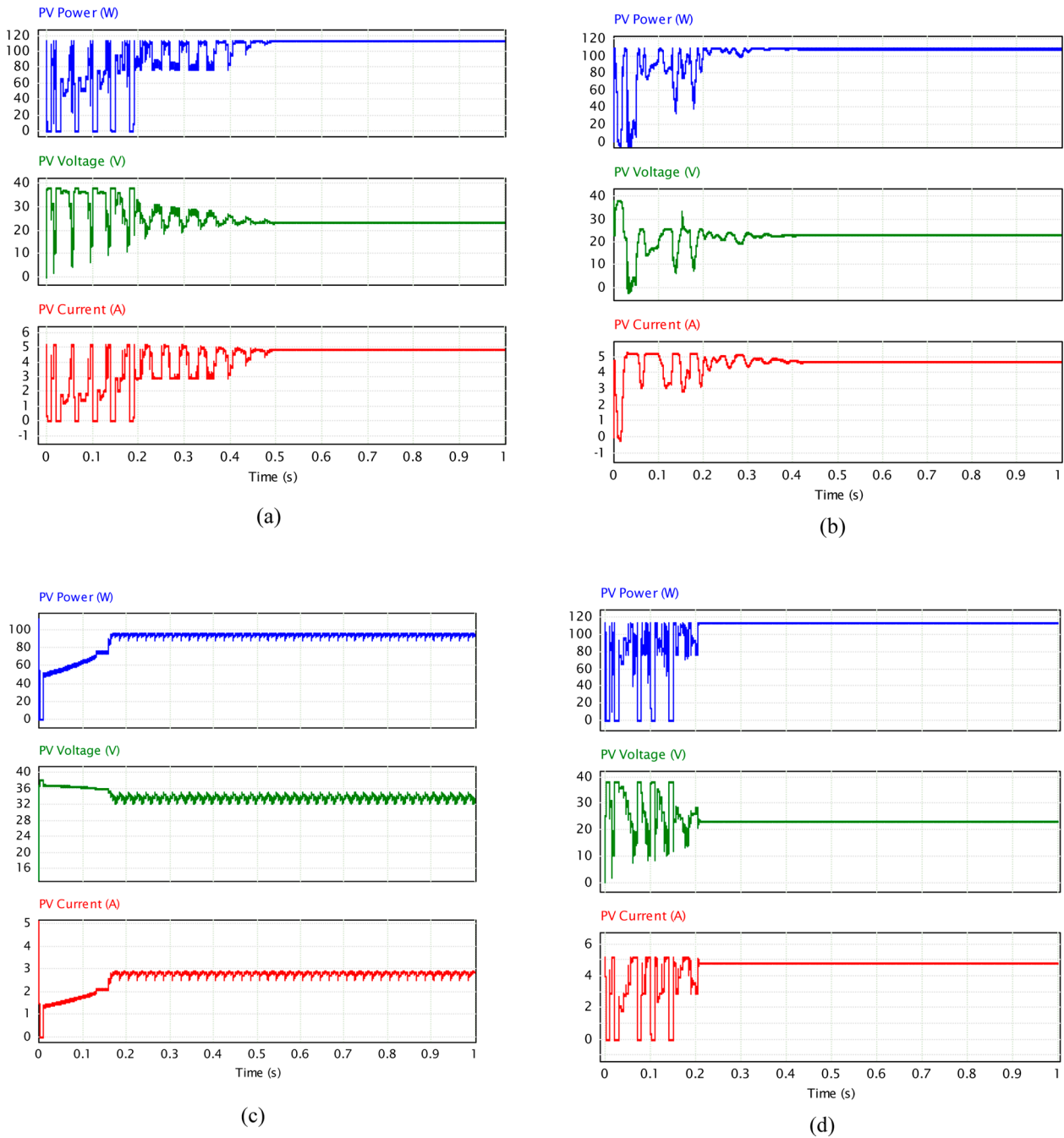
Figure 14. PV array output voltage, current and power waveforms for pattern 3: (a) GWO, (b) EGWO [35], (c) NGWO and (d) P&O.

Table 5. Comparison Variable swarm optimization methods with different swarm sizes and the number of peaks were tested in a simulation.

Methods	Swarm size	1 Peak		5 Peaks		10 Peaks		Average	
		FR	Conv.time	FR	Conv.time	FR	Conv.time	FR	Conv.time
GWO	3	0	0.35	14	0.41	24	0.44	12.67	0.40
EGWO		0	0.3	15	0.32	30	0.39	15	0.33
NGWO		0	0.15	11	0.18	22	0.21	11	0.18
GWO	4	0	0.4	6	0.47	19	0.48	8.34	0.45
EGWO		0	0.36	10	0.46	16	0.49	8.67	0.44
NGWO		0	0.19	0	0.23	11	0.34	3.67	0.25
GWO	6	0	0.53	0	0.57	10	0.66	3.34	0.58
EGWO		0	0.48	0	0.53	12	0.58	4	0.53
NGWO		0	0.31	0	0.38	0	0.44	0	0.37
GWO	8	0	0.68	0	0.71	0	0.75	0	0.71
EGWO		0	0.64	0	0.68	0	0.73	0	0.69
NGWO		0	0.44	0	0.5	0	0.52	0	0.49
GWO	10	0	0.77	0	0.80	0	0.82	0	0.79
EGWO		0	0.70	0	0.80	0	0.84	0	0.78
NGWO		0	0.49	0	0.51	0	0.56	0	0.52
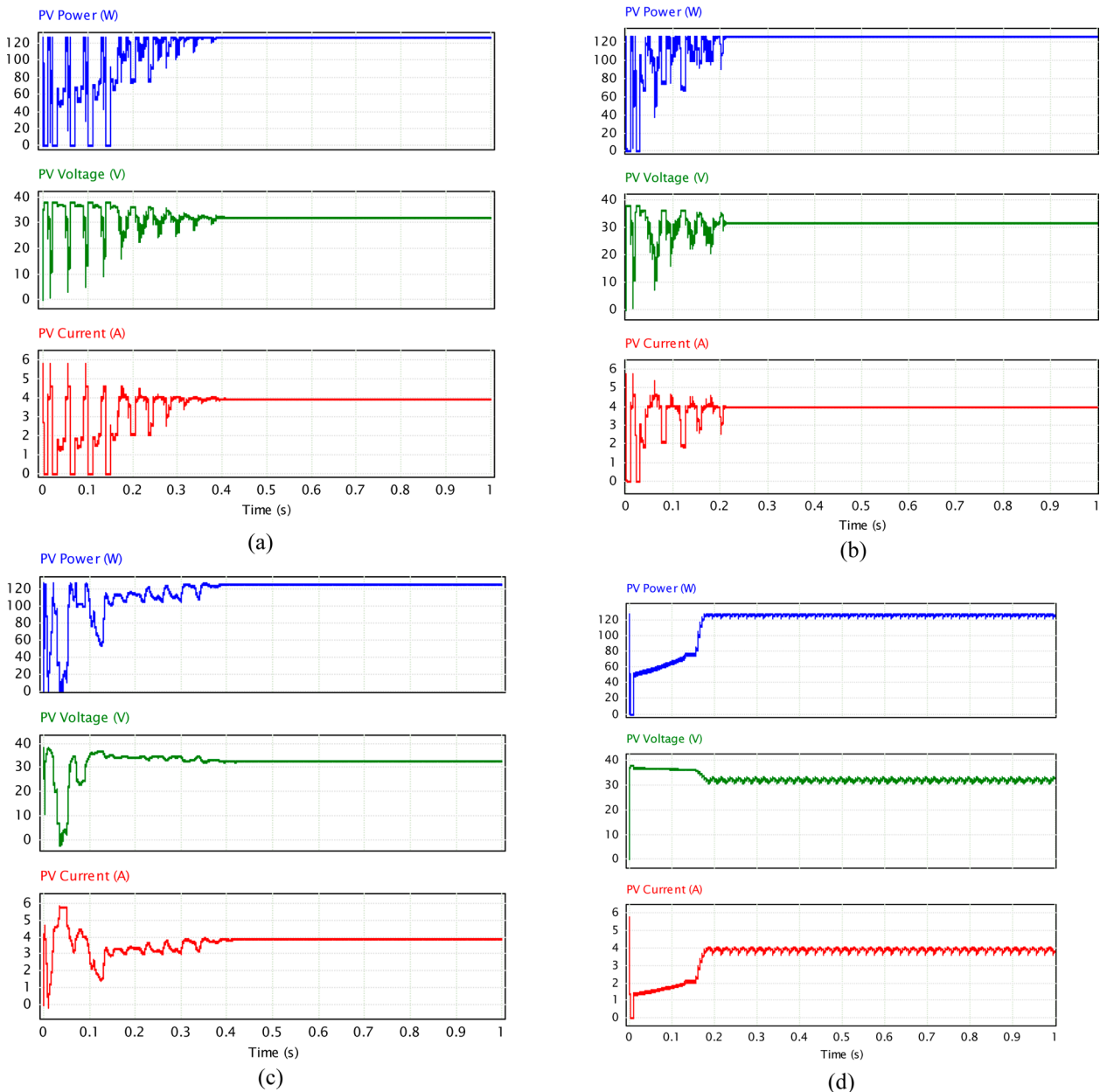
Figure 15. PV array output voltage, current and power waveforms for pattern 4: (a) GWO, (b) EGWO [35], (c) NGWO and (d) P&O.

If there are 10 peaks, NGWO was the only method that could capture the GMPP with a 0% FR using six searching agents. Additionally, it had the fastest conversion time of all the methods. When searching agents are 8 or higher, the FR was 0%. This indicates that the value of FR is higher than 0, which can be assigned to, GWO and EGWO under the case of 3, 4 and 6 searching agents, excluding the case with 8 and 10 searching agents.

With 8 searching agents, all optimization methods achieved an FR with the rate of 0%; the NGWO was able to capture the GMPP in 0.52 s, while the GWO and EGWO took 0.75 and 0.73 s, respectively.

When the number 10 of searching agents was used, GWO, EGWO and NGWO successfully caught the GMPP at 0% FR; however, NGWO had the fastest convergence speed. This proves, once more,

that the NGWO has a better performance compared to the GWO and EGWO that were utilized in this study.

In addition, the average results across all of the evaluated numbers of peaks are displayed in Table 5. It is abundantly evident that the average rates of failure for all optimization methods for three and four searching agents are greater than 0%. NGWO is the only technique to attain an FR of 0% with six searching agents, while GWO and EGWO have FRs of 4% and 3%, respectively. Compared with the average convergence times associated with other optimization methods, NGWO is noticeably faster across the board, regardless of the number of various search agents that were employed. The results of this study show that the NGWO method outperforms all of the other MPPT methods that were examined for use with PV systems.
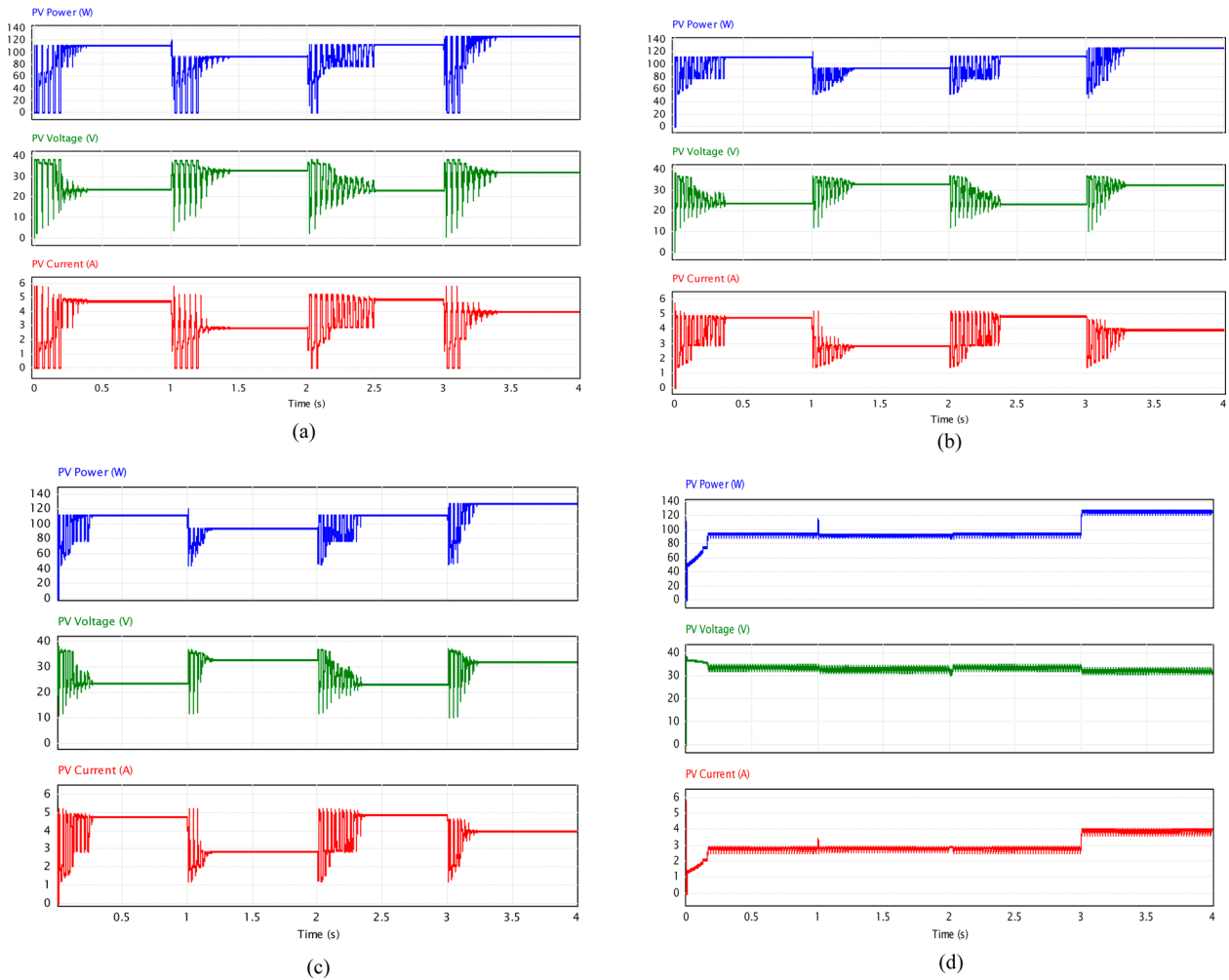
Figure 16. Dynamic performance under PSC changes: (a) GWO, (b) EGWO [35], (c) NGWO and (d) P&O.
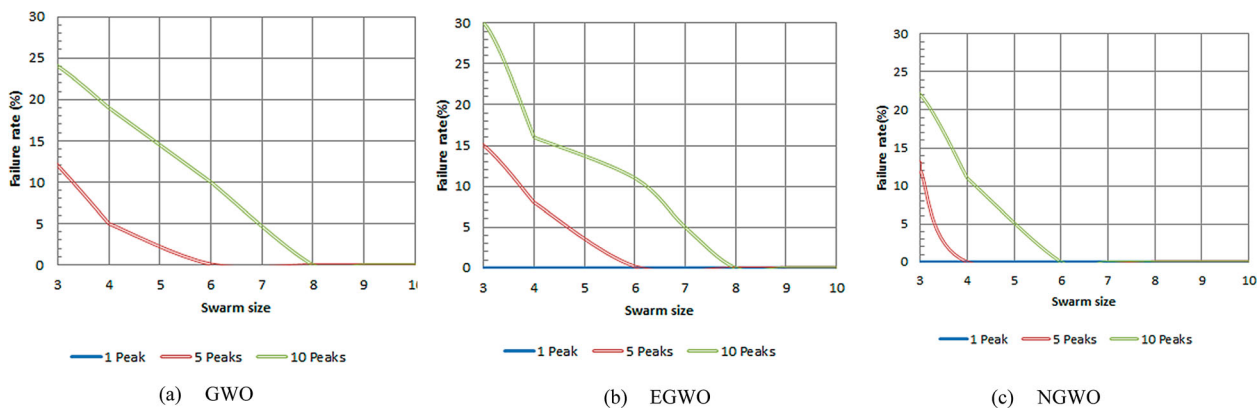
Figure 17. Shows a visual representation of how the failure rate varied as the swarm size increased and with different number of peaks for all optimization methods. (a) GWO; (b) EGWO; (c) NGWO.

Figure 17 shows the variation in swarm size and failure rate for optimization methods that were tested.

Figure 18 shows the variation in swarm size and convergence time for optimization methods that were tested.

6. Conclusion

This paper proposes a novel Grey Wolf Optimization (GWO) algorithm designed for use in photovoltaic (PV) systems, capable of tracking the Global Maximum Power Point (GMPP) under various partial shading conditions (PSCs). The abandonment mechanism from Cuckoo Search (CS) is utilized to enhance the performance of the GWO-based Maximum Power Point Tracking (MPPT) by reducing tracking time and improving efficiency through the retention of high-quality solutions and the discarding of low-quality ones. Extensive simulation studies were conducted to demonstrate that the proposed Novel Grey Wolf
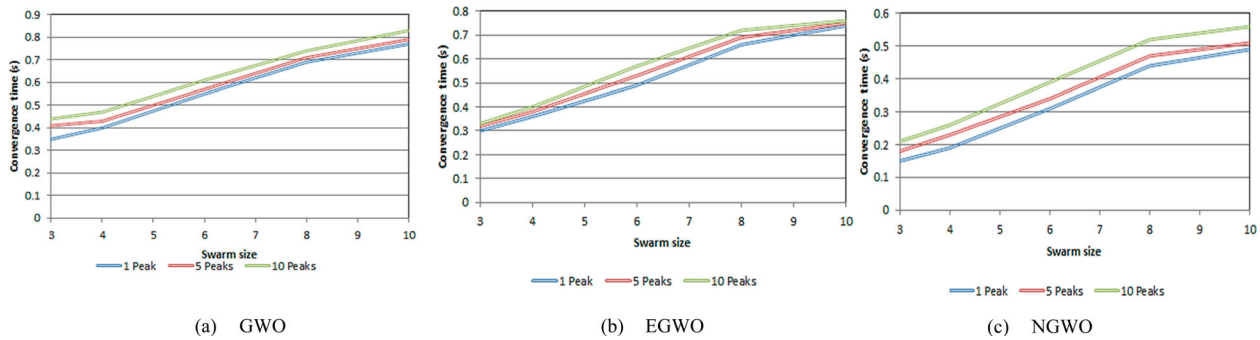
Figure 18. Shows a visual representation of how the convergence time varied as the swarm size increased and with different number of peaks for all optimization methods. (a) GWO; (b) EGWO; (c) NGWO.

Optimization (NGWO) is both feasible and effective. A numerical analysis of each optimization method's performance was presented, using a wide range of P–V curve peak numbers and swarm sizes. The performance of the NGWO algorithm was compared with the traditional GWO, the Enhanced GWO (EGWO) and the Perturb & Observe (P&O) algorithm. Moreover, the results of the MPPT tests conducted on PV system simulation software confirmed the effectiveness of the proposed NGWO algorithm. The findings indicated that the NGWO algorithm outperformed other algorithms in terms of speed of convergence, low failure rate, minimal oscillations during convergence and overall tracking efficiency.

Disclosure statement

No potential conflict of interest was reported by the author(s).

ORCID

Muhannad J. Alshareef http://orcid.org/0000-0002-0390-7412

References

[1] Alshareef MJ. An effective falcon optimization algorithm based MPPT under partial shaded photovoltaic systems. IEEE Access. 2022;10:131345–131360. doi:10.1109/ACCESS.2022.3226654

[2] Gündoğdu HA. System identification based ARV-MPPT technique for PV systems under variable atmospheric conditions. in IEEE Access. 2022;10:51325–51342. doi:10.1109/ACCESS.2022.3174107

[3] Khodair D, Motahhir S, Mostafa HH, et al. Modeling and simulation of modified MPPT techniques under varying operating climatic conditions. Energies. 2023;16(1):549. doi:10.3390/en16010549

[4] Devarakonda AK, Karuppiah N, Selvaraj T, et al. A comparative analysis of maximum power point techniques for solar photovoltaic systems. Energies. 2022;15(22):8776. doi:10.3390/en15228776

[5] Noguchi T, Togashi S, Nakamoto R. Short-current pulse-based maximum-power-point tracking method for multiple photovoltaic-and-converter module system. IEEE Trans Ind Electron. Feb 2002;49(1):217–223. doi:10.1109/41.982265

[6] Baimel D, Tapuchi S, Levron Y, et al. Improved fractional open circuit voltage MPPT methods for PV systems. Electronics (Basel). 2019;8(3):321. doi:10.3390/electronics8030321

[7] Manoharan P, Subramaniam U, Babu TS, et al. Improved perturb and observation maximum power point tracking technique for solar photovoltaic power generation systems. IEEE Syst J. June 2021;15(2):3024–3035. doi:10.1109/JSYST.2020.3003255

[8] Alajmi BN, Ahmed KH, Finney SJ, et al. Fuzzy-logic-control approach of a modified hill-climbing method for maximum power point in microgrid standalone photovoltaic system. IEEE Trans Power Electron. April 2011;26(4):1022–1030. doi:10.1109/TPEL.2010.2090903

[9] Roy RB, Rokonuzzaman Md., Amin N, et al. A comparative performance analysis of ANN algorithms for MPPT energy harvesting in solar PV system. IEEE Access. 2021;9:102137–102152. doi:10.1109/ACCESS.2021.3096864

[10] Podder AK, Roy NK, Pota HR. MPPT methods for solar PV systems: a critical review based on tracking nature. IET Renew Power Gener. 2019;13(10):1615–1632. doi:10.1049/iet-rpg.2018.5946

[11] Alshareef M, Lin Z, Ma M, et al. Accelerated particle swarm optimization for photovoltaic maximum power point tracking under partial shading conditions. Energies. 2019;12(4):623. doi:10.3390/en12040623

[12] Ishaque K, Salam Z, Amjad M, et al. An improved particle swarm optimization (PSO)–based MPPT for PV with reduced steady-state oscillation. IEEE Trans Power Electron. Aug 2012;27(8):3627–3638. doi:10.1109/TPEL.2012.2185713

[13] Gopalakrishnan SK, Kinattingal S, Simon SP, et al. Enhanced energy harvesting from shaded PV systems using an improved particle swarm optimisation. IET Renew Power Gener. 2020;14(9):1471–1480. doi:10.1049/iet-rpg.2019.0936

[14] Sundareswaran K, Peddapati S, Palani S. MPPT of PV systems under partial shaded conditions through a colony of flashing fireflies. IEEE Trans Energy Convers. June 2014;29(2):463–472. doi:10.1109/TEC.2014.2298237

[15] Sundareswaran K, Sankar P, Nayak PS, et al. Enhanced energy output from a PV system under partial shaded conditions through artificial bee colony. IEEE Trans Sustain Energy. 2015;6(1):198–209. doi:10.1109/TSTE.2014.2363521

[16] Mohanty S, Subudhi B, Ray PK. A new MPPT design using grey wolf optimization technique for photovoltaic system under partial shading conditions.

IEEE Trans Sustain Energy. Jan 2016;7(1):181–188. doi:10.1109/TSTE.2015.2482120

[17] Kaced K, Larbes C, Ramzan N, et al. Bat algorithm based maximum power point tracking for photovoltaic system under partial shading conditions. Sol Energy. 2017;158:490–503. doi:10.1016/j.solener.2017.09.063

[18] Liu Y-H, Huang S-C, Huang J-W, et al. A particle swarm optimization-based maximum power point tracking algorithm for PV systems operating under partially shaded conditions. IEEE Trans Energy Convers. Dec 2012;27(4):1027–1035. doi:10.1109/TEC.2012.2219533

[19] Qi P, Xia H, Cai X, et al. Novel global MPPT technique based on hybrid cuckoo search and artificial bee colony under partial-shading conditions. Electronics (Basel). Apr 2024;13(7):1337. doi:10.3390/electronics13071337

[20] Chtita S, Motahhir S, El Hammoumi A, et al. A novel hybrid GWO–PSO-based maximum power point tracking for photovoltaic systems operating under partial shading conditions. Sci Rep. Jun 2022;12(1):10637. doi:10.1038/s41598-022-14733-6

[21] Kermadi M, Salam Z, Ahmed J, et al. An effective hybrid maximum power point tracker of photovoltaic arrays for complex partial shading conditions. IEEE Trans Ind Electron. Sept 2019;66(9):6990–7000. doi:10.1109/TIE.2018.2877202

[22] Chao K-H, Li J-Y. Global maximum power point tracking of photovoltaic module arrays based on improved artificial bee colony algorithm. Electronics (Basel). May 2022;11(10):1572. doi:10.3390/electronics11101572

[23] Dhieb Y, Yaich M, Bouzguenda M, et al. MPPT optimization using ant colony algorithm: solar PV applications. In 2022 IEEE 21st international conference on sciences and techniques of automatic control and computer engineering (STA), Sousse, Tunisia; 2022. p. 503–507.

[24] Tey KS, Mekhilef S, Seyedmahmoudian M, et al. Improved differential evolution-based MPPT algorithm using SEPIC for PV systems under partial shading conditions and load variation. IEEE Trans Ind Informat. Oct 2018;14(10):43224333.

[25] Guo K, Cui L, Mao M, et al. An improved gray wolf optimizer MPPT algorithm for PV system with BFBIC converter under partial shading. IEEE Access. 2020;8:103476–103490. doi:10.1109/ACCESS.2020.2999311

[26] Wang M, Gao B. An improved GWO technique integrated with P&O algorithm for photovoltaic system considering different conditions in the irradiance. In 2022 IEEE 5th international electrical and energy conference (CIEEC), Nangjing, People's Republic of China; 2022. p. 1013–1018.

[27] Mittal N, Singh U, Sohi BS. Modified grey wolf optimizer for global engineering optimization. In: Proc. Appl. Comput. Intell. Soft Comput., 2016, vol. 2016. p. 1–16.

[28] Wan Y, Mao M, Zhou L, et al. A novel nature-inspired maximum power point tracking (MPPT) controller based on SSA-GWO algorithm for partially shaded photovoltaic systems. Electronics (Basel). 2019;8(6):680. doi:10.3390/electronics8060680

[29] Davoodkhani F, Arabi Nowdeh S, Abdelaziz AY, et al. A new hybrid method based on Gray Wolf optimizer-crow search algorithm for maximum power point tracking of Photovoltaic Energy System. In: Modern maximum power point tracking techniques for photovoltaic energy systems; 2019. p. 421–438.

[30] Pai F-S, Tseng P-S. An efficient GWO MPPT for a PV system using impedance information acceleration. Int J Electron. 2018;106(4):648–661. doi:10.1080/00207217.2018.1545929

[31] Yang X-S, Deb S. Cuckoo search via Lévy flights. In: 2009 world congress on nature & biologically inspired computing (NaBIC), Coimbatore, India; 2009. p. 210–214.

[32] Peng B-R, Ho K-C, Liu Y-H. A novel and fast MPPT method suitable for both fast changing and partially shaded conditions. IEEE Trans Ind Electron. April 2018;65(4):3240–3251. doi:10.1109/TIE.2017.2736484

[33] Ahmed JJ, Salam Z. An enhanced adaptive P&O MPPT for fast and efficient tracking under varying environmental conditions. EEE Trans Sustain Energy. July 2018;9(3):1487–1496. doi:10.1109/TSTE.2018.2791968

[34] Ahmed J, Salam Z. A maximum power point tracking (MPPT) for PV system using cuckoo search with partial shading capability. Appl Energy. Apr 2014;119:118–130. doi:10.1016/j.apenergy.2013.12.062

[35] Cherukuri SK, Rayapudi SR. Enhanced grey wolf optimizer based MPPT algorithm of PV system under partial shaded condition. Int J Renew Energy Dev. 2017;6(3):203. doi:10.14710/ijred.6.3.203-212

[36] Laudani A, Fulginei FR, Salvini A. Identification of the one-diode model for photovoltaic modules from datasheet values. Sol Energy. 2014;108:432–446. doi:10.1016/j.solener.2014.07.024

[37] Huang Y-P, Hsu S-Y. A performance evaluation model of a high concentration photovoltaic module with a fractional open circuit voltage-based maximum power point tracking algorithm. Comput Electr Eng. 2016;51:331–342. doi:10.1016/j.compeleceng.2016.01.009

[38] Li G, Jin Y, Akram MW, et al. Application of bio-inspired algorithms in maximum power point tracking for PV systems under partial shading conditions – a review. Renewable Sustainable Energy Rev. 2018;81:840–873. doi:10.1016/j.rser.2017.08.034

[39] Mirjalilim S, Mirjalili SM, Lewis A. Grey wolf optimizer. Adv. Eng. Software. 2014;69:46–61. doi:10.1016/j.advengsoft.2013.12.007

[40] Liao C Y, Subroto R K, Millah I S, et al. An Improved Bat Algorithm for More Efficient and Faster Maximum Power Point Tracking for a Photovoltaic System Under Partial Shading Conditions. IEEE Access; 2020-01. p. 96378–96390. doi:10.1109/access.2020.2993361